Operator-Based Uncertainty Quantification of Stochastic Fractional PDEs

Ehsan Kharazmi
Department of Mechanical Engineering &
Department of Computational Mathematics, Science, and Engineering
Michigan State University
428 S Shaw Lane, East Lansing, MI 48824, USA
Email: kharazm2@msu.edu

Mohsen Zayernouri*
Department of Mechanical Engineering &
Department of Computational Mathematics, Science, and Engineering
Michigan State University
428 S Shaw Lane, East Lansing, MI 48824, USA
Email: zayern@egr.msu.edu

Fractional calculus provides a rigorous mathematical framework to describe anomalous stochastic processes by generalizing the notion of classical differential equations to their fractional-order counterparts. By introducing the fractional orders as uncertain variables, we develop an operator-based uncertainty quantification framework in the context of stochastic fractional partial differential equations (SFPDEs), subject to additive random noise. We characterize different sources of uncertainty and then, propagate their associated randomness to the system response by employing a probabilistic collocation method (PCM). We develop a fast, stable, and convergent Petrov-Galerkin spectral method in the physical domain in order to formulate the forward solver in simulating each realization of random variables in the sampling procedure.

1 Introduction

Fractional models construct a tractable mathematical framework to describe and predict the behavior of multi-scales multi-physics complex phenomena. Particularly, fractional differential equations, as a well-structured generalization of their integer order counterparts, provide a rigorous mathematical tool to develop models that describe anomalous behavior in complex physical systems [1–9], where the anomaly manifest itself in heavy tail, sharp peaks, intermittency and asymmetry in the distribution of corresponding underlying stochastic processes. Significant approximations as inherent part of assumptions upon which the model is built, lack of information about true values of parameters (incomplete data), and random nature of quantities being modeled pervade uncertainty in the corresponding mathematical formulations [10, 11]. In this work, we develop an uncertainty quantification (UQ) framework in the context of stochastic fractional partial differential equations (SFPDEs), in which we characterize different sources of uncertainties and further propagate the associated randomness to the system response quantity of interest (QoI). The intention of this work is not to introduce new mathematical theories or methods for UQ, but rather to bring forward practical solutions using existing theories in an attempt to overcome the computational challenges of UQ in fractional models.

Types and Sources of Uncertainty. The model uncertainties are in general being classified as aleatory and epistemic according to their fundamental essence. It is important to retain the separation between these two sources in order to assess the predictive efficiency of model [12, 13]. Aleatory uncertainty impacts output of interest due to natural variation of inputs and parameters; it is irreducible and commonly treated with probability theory. Epistemic uncertainty, however, results from lack of knowledge about the system of interest and can be reduced by obtaining additional information. The epistemic uncertainties are broadly characterized as *i)* model uncertainties, occurring in model inputs, numerical approximation errors, and model form uncertainty; and *ii)* data uncertainties due to measurement inaccuracy and sparse or imprecise data. The model uncertainty encompasses all model parameters coming from geometry, constitutive laws, and fields equation, while also pertaining surrounding interactions, such as boundary conditions and random forcing sources (noise). Numerical approximations, which are an essence of differential equations since they generally do not

*Corresponding author.

lend themselves to analytical solutions, introduce uncertainty by imposing different sources of discretization error, iterative convergence error, and round off error. In this work, we only consider the epistemic uncertainty in our fractional model and thus, introduce the fractional derivative orders as new set of model parameters in addition to model coefficients. We note that the values of these new parameters are strongly tied to the distribution of underlying stochastic process and their statistics are estimated from experimental observations in practice, see e.g. [14, 15].

Uncertainty Framework. Conventional approaches in parametric UQ of differential equations is based around Monte Carlo sampling (MCS) [16], which performs ensemble of forward calculations to map the uncertain input space to the uncertain output space. This method enjoys from being embarrassingly parallelizable and can be implement quite readily on high dimensional random spaces. However, the key issue is the slow rate of convergence $\sim 1/\sqrt{N}$ with N number of realization, which consequently imposes exhaustively so many operations of forward solver and makes the method not practical for expensive simulations. Other methods such as sequential MCS [17] and multilevel sequential MSC [18] are also developed and recently used in [19] to improve the parametric uncertainty assessment in elliptic nonlocal equations. An alternative to expensive MCS is to build surrogate models. An extensive comparison of two widely used ones, namely polynomial chaos and Gaussian process, are provided in a recent work [20]. Polynomial chaos, in which the output of stochastic model is represented as a series expansion of input parameters was initially applied in [21] and later extended and used in [22–26]. It is also generalized and used in constructing stochastic Galerkin methods [27–30] for problems with higher-dimensional random spaces. Other non-sampling numerical methods, including but not limited to perturbation method [31–34] and moment equation method [35, 36] are also developed, however their applications are restricted to stochastic systems with relatively low-dimensional random space. These so-called "*intrusive*" approaches typically do not treat the forward solver as a black-box, rather require some knowledge and reformulation of the governing equations and thus, may not be practical in many problems with complex codes.

A wide range of "*non-intrusive*" techniques mostly stretch over sampling, quadrature, and regression, see [20] and references therein. More recently, high-order probabilistic collocation methods (PCM), employing the idea of interpolation/collocation in the random spaces, are developed in [37–39]; They are also known as Stochastic Collocation. These methods limit the sample points to an efficient subset of random space, while adequately sampling the necessary range. The excellence in use of PCM is twofold; it has the benefit of easily sampling at nodal points that naturally leads to independent realizations of the problem as in MCS, and the advantage of fast convergence rate. The challenging post processing of solution statistics, which can essentially be described as a high-dimensional integration problem, can also be resolved by adopting sparse grid generators, such as Smolyak algorithm [39, 40]. The use of sparse grids, as opposed to full tensor product construction from one-dimensional quadrature rules, will effectively reduce the number of sampling, while preserving a fast convergence rate to high level of accuracy.

Forward Solver. A core task in computational forward UQ is to form an efficient numerical method, which for each realizations of random variables can accurately solve and simulate the deterministic counterpart of stochastic model in the physical domain. Such numerical method is usually called "*forward solver*" or "*simulator*". In the case of fractional partial differential equations (FPDEs), the excessive cost of numerical approximations becomes more challenging as FPDEs usually do not lend themselves to analytical solutions and more importantly most of uncertainty propagation techniques instruct operations of forward solver many times. This requires implementation of more efficient numerical schemes. In general, there are two main issues of *nonlocality* and *end-points singularities* in numerically solving FPDEs. The non-local feature of fractional derivatives causes the local methods such as finite difference method (FDM) and finite element method (FEM) to lose their advantage, see [41–48] for some examples on FDM for solving FPDEs. In contrast, global and high-order schemes like spectral methods are proper techniques since their main disadvantage in treating standard differential equations becomes an advantage in the case of FPDEs. We refer to [57, 58] for introduction to several spectral methods for integer order differential equation and to [43, 49–56] for FPDEs. The solution of FPDEs also exhibits end-points singularities as another difficulty in developing high accuracy numerical methods; An example is the inadequacy of a spectral method that uses only polynomial basis functions. More recently, Zayernouri et al. [59, 60] developed two new spectral theories on fractional and tempered fractional Sturm-Liouville problems, and introduced explicit corresponding eigenfunctions, namely *Jacobi poly-fractonomials* of first and second kind. These eignefunctions are comprised of smooth and fractional parts, where the latter can be tunned to capture singularities of true solution. They are successfully employed in constructing discrete solution/test function spaces and developing a series of high-order and efficient Petrov-Galerkin spectral methods, see [61–72].

The main focus of this work is to develop an operator-based computational forward UQ framework in the context of stochastic fractional partial differential equation. Assuming that the mathematical model under consideration is well-posed and accounts in principle for all features of underlying phenomena, we identify three main sources of uncertainty, *i*) parametric uncertainty, including fractional indices as new set of random parameters appeared in the operator, *ii*) additive noises, which incorporates all intrinsic/extrinsic unknown forcing sources as lumped random inputs, and *iii*) numerical approximations. Computational challenges arise when the admissible space of random inputs is infinite-dimensional, e.g. problems subject to addi-

tive noise [73], and thus, the framework involves uncertainty parametrization via a finite number of random space basis. Unlike the classical approach in modeling random inputs, which considers idealized uncorrelated processes (white noises), we model the random inputs as more/fully correlated random processes (colored noises), and parametrize them via Karhunen-Loève (KL) expansion by assuming finite-dimensional noise assumption. This yields the problem in finite dimensional random space. We then, propagate the parametric uncertainties into the system response by applying PCM. We obtain the corresponding deterministic FPDE for each realization of random variables, using the Smolyak sparse grid generators for low to moderately high dimensions. In order to formulate the forward solver, we follow [65] and develop a high-order Petrov-Galerkin (PG) spectral method to solve for each realization of SFPDE in the physical domain by employing Jacobi poly-fractonomials in addition to Legendre polynomials as temporal and spatial basis/test functions, respectively. The smart choice of coefficients in construction of spatial basis/test functions yields symmetric properties in the resulting mass/stiffness matrix, which is then exploited to formulate an efficient fast solver. We also show that for each realization of random variables, the deterministic problem is mathematically well-posed and the proposed forward solver is stable. By adopting sufficient number of basis in the physical domain, we eliminate the epistemic uncertainty associated with numerical approximation and isolate the impact of parametric uncertainty on system response QoI.

The organization of the paper is as follows. We recall some preliminaries on fractional calculus in section 2. Then, we formulate the stochastic system in section 3, and parametrize the random inputs. We also develop the stochastic sampling, namely PCM and MCS for our stochastic problem. We further construct the deterministic solver in section 4, and provide the numerical results in section 5. We end the paper with a conclusion and summary.

2 Preliminaries on Fractional Calculus

Let $\xi \in [-1,1]$. The left- and right-sided fractional derivative of order σ are defined as (see e.g., [74, 75])

$$({}^{RL}_{-1}\mathcal{D}^{\sigma}_{\xi})u(\xi) = \frac{1}{\Gamma(n-\sigma)}\frac{d^n}{d\xi^n}\int_{-1}^{\xi}\frac{u(s)ds}{(\xi-s)^{\sigma+1-n}}, \quad \xi > -1, \tag{1}$$

$$({}^{RL}_{\xi}\mathcal{D}^{\sigma}_{1})u(\xi) = \frac{1}{\Gamma(n-\sigma)}\frac{(-d)^n}{d\xi^n}\int_{\xi}^{1}\frac{u(s)ds}{(s-\xi)^{\sigma+1-n}}, \quad \xi < 1, \tag{2}$$

respectively. An alternative approach in defining the fractional derivatives is the left- and right-sided Caputo derivatives of order σ, $n-1 < \sigma \le n$, $n \in \mathbb{N}$, defined, as

$$({}^{C}_{-1}\mathcal{D}^{\sigma}_{\xi}u)(\xi) = \frac{1}{\Gamma(n-\sigma)}\int_{-1}^{\xi}\frac{u^{(n)}(s)ds}{(\xi-s)^{\sigma+1-n}}, \quad \xi > -1, \tag{3}$$

$$({}^{C}_{\xi}\mathcal{D}^{\sigma}_{1}u)(\xi) = \frac{1}{\Gamma(n-\sigma)}\int_{\xi}^{1}\frac{u^{(n)}(s)ds}{(s-\xi)^{\sigma+1-n}}, \quad \xi < 1. \tag{4}$$

By performing an affine mapping from the standard domain $[-1,1]$ to the interval $t \in [a,b]$, we obtain

$${}^{RL}_{a}\mathcal{D}^{\sigma}_{t}u = (\frac{2}{b-a})^{\sigma}({}^{RL}_{-1}\mathcal{D}^{\sigma}_{\xi}u)(\xi), \tag{5}$$

$${}^{C}_{a}\mathcal{D}^{\sigma}_{t}u = (\frac{2}{b-a})^{\sigma}({}^{C}_{-1}\mathcal{D}^{\sigma}_{\xi}u)(\xi). \tag{6}$$

Hence, we can perform the operations in the standard domain only once for any given σ and efficiently utilize them on any arbitrary interval without resorting to repeating the calculations. Moreover, the corresponding relationship between the Riemann-Liouville and Caputo fractional derivatives in $[a,b]$ for any $\sigma \in (0,1)$ is given by

$$({}^{RL}_{a}\mathcal{D}^{\sigma}_{t}u)(t) = \frac{u(a)}{\Gamma(1-\sigma)(t-a)^{\sigma}} + ({}^{C}_{a}\mathcal{D}^{\sigma}_{t}u)(t). \tag{7}$$

3 Forward Uncertainty Framework

3.1 Formulation of Stochastic FPDE

Let $\mathbb{D} = [0,T]\times[a_1,b_1]\times[a_2,b_2]\times\cdots\times[a_d,b_d]$ be the physical computational domain for some positive integer d and stochastic function $u(t,\mathbf{x};\omega) : \mathbb{D}\times\Omega \to \mathbb{R}$, where $\omega \in \Omega$ denotes the random input of the system in a properly defined complete probability space $(\Omega,\mathcal{F},\mathbb{P})$. We consider the following SFPDE, subject to certain homogeneous Dirichlet initial/boundary conditions and stochastic process as additional force function, given as

$$\mathcal{L}^{q(\omega)}u(t,\mathbf{x};\omega) = F(t,\mathbf{x};\omega) \tag{8}$$

$$u\,|_{t=0} = 0, \tag{9}$$

$$u\,|_{x=a_j} = u\,|_{x=b_j} = 0, \tag{10}$$

such that for $\mathbb{P}$-almost everywhere $\omega \in \Omega$ the equation holds. The stochastic fractional operator and force term are given respectively as:

$$\mathcal{L}^{q(\omega)} = {}_0\mathcal{D}^{\alpha(\omega)}_{t} - \sum_{j=1}^{d} k_j\left[{}_{a_j}\mathcal{D}^{\beta_j(\omega)}_{x_j} + {}_{x_j}\mathcal{D}^{\beta_j(\omega)}_{b_j}\right], \tag{11}$$

$$F(t,\mathbf{x};\omega) = h(t,\mathbf{x}) + f(t;\omega), \tag{12}$$

where the fractional indices $\alpha(\omega) \in (0,1)$ and $\beta_j(\omega) \in (1,2)$, $j = 1,2,\cdots d$ are mutually independent random variables, k_j are real positive constant coefficients, and the fractional derivatives are taken in the Riemann-Liouville sense.

We assume that the driving terms h and f are properly posed, such that Eqns. (8)-(10) is well-posed $\mathbb{P}$-a.e. $\omega \in \Omega$, and also the solution in physical domain $\mathbb{D}$ is smooth enough such that we can construct a numerical scheme to solve each realization of SFPDE. As an extension to future works, the stochastic operator Eqn. (11) can be extended to $\alpha(\omega) \in (1,2)$ for the case of wave equations, and thus applied in formulating fractional models to study complex time-varying nonlinear fluid-solid interaction phenomena [76–78], material damage [79], and also the effect of damping/stiffness in structural vibrations [80–83].

3.2 Representation of the Noise: Dimension Reduction

We approximate the additional random forcing term by representing $f(t;\omega)$ into its finite dimensional version and thus, reduce the infinite-dimensional probability space to a finite-dimensional space. This is achieved via truncating Karhunen-Loève (KL) expansion with the desired accuracy [84].

Let $(\Omega, \mathcal{F}, \mathbb{P})$ be a complete probability space, where Ω is the space of events, $\mathcal{F} \subset 2^{\Omega}$ denotes the σ-algebra of sets in Ω, and $\mathbb{P}$ is the probability measure. The random field $f(t;\omega)$ has the ensemble mean $\mathbb{E}\{f(t;\omega)\} = \bar{f}(t)$, finite variance $\mathbb{E}\{[f(t;\omega) - \bar{f}(t)]^2\}$ and covariance $C_f(t_1,t_2) = \mathbb{E}\{[f(t_1;\omega) - \bar{f}(t_1)][f(t_2;\omega) - \bar{f}(t_2)]\}$. The KL expansion of $f(t;\omega)$ takes the form

$$f(t;\omega) = \bar{f}(t) + \sum_{k=1}^{\infty} \sqrt{\lambda_k}\,\psi_k(t)\,Q_k(\omega), \tag{13}$$

where $\boldsymbol{Q}(\omega) = \{Q_k(\omega)\}\big|_{k=1}^{k=\infty}$ is a set of mutually uncorrelated random variables with zero mean and unit variance, while $\psi_k(t)$ and λ_k are the eigenfunction and eigenvalues of the covariance kernel $C_f(t_1,t_2)$. We obtain the covariance kernel C_f and its eigenvalues and eigenfunctions, following [85] and by solving a stochastic Helmholtz equation

$$\triangle f(t;\omega) - m^2 f(t;\omega) = g(t;\omega), \tag{14}$$

where the random forcing $g(t;\omega)$ is a white-noise process with zero mean and unit variance. The eigenvalues and eigenvectors of Eqn. (14) form a Fourier series, so that the KL expansion Eqn. (13) is replaced with its sine Fourier series version

$$f(t;\omega) = \bar{f}(t;\omega) + \sum_{k=1}^{\infty} a_k \sin\left(\frac{2k\pi t}{T}\right) Q_k(\omega), \tag{15}$$

in which the random variables $Q_k(\omega)$ are chosen to be *uniformly* distributed with probability density function $\rho_k(q_k)$. T is the length of the process along the t-axis, and the coefficients

$$a_k = \frac{2}{\sqrt{T}\ell^2}\left[1 + \left(\frac{2\pi k}{T\ell}\right)^2\right]^{-1}, \tag{16}$$

where $\ell = T/A$ and A is the correlation length of $f(t;\omega)$. To ensure that the random variables $Q_k(\omega)$ have zero mean and unit variance, we define them on $Q_k(\omega) \in [-\sqrt{3}, \sqrt{3}]$. We note that this process is consistent to the zero-Dirichlet initial condition given in Eqn. (9). Next, in order to render Eqn. (15) computable, we truncate the infinite series with a prescribed ($\approx 90\%$) fraction of the energy of the process, following the finite-dimensional noise assumption in stochastic computations. To this end, we set $T = 1$, the correlation length $A = T/2$, and consider only the first four terms in the KL expansion. Let $f_M(t;\omega) = \frac{1}{\mu}\sum_{k=1}^{M} a_k \sin\left(\frac{2k\pi t}{T}\right) Q_k(\omega)$ denote the normalized truncated expansion, assuming $\bar{f}_M(t;\omega) = 0$, where $\mu = \max_t\{\sigma_{f_M}\}$ and σ_{f_M} is the standard deviation of $f_M(t;\omega)$. Thus, we represent the random process to be employed in Eqn. (8) as

$$f(t;\omega) = \epsilon f_M(t;\omega) \tag{17}$$

where ϵ is the amplitude of process.

Therefore, the formulation of SFPDE Eqn. (8) can be posed as follows: Find $u(t,\mathbf{x};\omega) : \mathbb{D}\times\Omega \to \mathbb{R}$ such that $\forall t, \mathbf{x} \in \mathbb{D}$

$$\begin{aligned} &{}_0\mathcal{D}_t^{\alpha(\omega)} u(t,\mathbf{x};\omega) - \sum_{j=1}^{d} k_j \left[{}_{a_j}\mathcal{D}_{x_j}^{\beta_j(\omega)} + {}_{x_j}\mathcal{D}_{b_j}^{\beta_j(\omega)} \right] u(t,\mathbf{x};\omega) \\ &= h(t,\mathbf{x}) + f(t; Q_1(\omega), Q_2(\omega), \cdots, Q_M(\omega)) \end{aligned} \tag{18}$$

holds $\mathbb{P}$-a.s. for $\omega \in \Omega$, subject to the homogeneous initial and boundary conditions.

3.3 Input Parametrization

Let $Z : \Omega \to \mathbb{R}^{\mathcal{N}}$ be the set of $\mathcal{N} = 1 + d + M$ independent random parameters, given as

$$\begin{aligned} Z &= \left\{Z_i\right\}_{i=1}^{\mathcal{N}} \\ &= \left\{\alpha(\omega), \beta_1(\omega), \beta_2(\omega), \cdots, \beta_d(\omega), Q_1(\omega), Q_2(\omega), \cdots, Q_M(\omega)\right\} \end{aligned}$$

with probability density functions $\rho_i : \Gamma_i \to \mathbb{R}$, $i = 1, 2, \cdots, \mathcal{N}$, where their images $\Gamma_i \equiv Z_i(\Omega)$ are bounded intervals in $\mathbb{R}$. The joint probability density function (PDF)

$$\rho(\boldsymbol{\xi}) = \prod_{i=1}^{\mathcal{N}} \rho_i(Z_i), \quad \forall \boldsymbol{\xi} \in \Gamma \tag{19}$$

with the support $\Gamma = \prod_{i=1}^{\mathcal{N}} \Gamma_i \subset \mathbb{R}^{\mathcal{N}}$ constitutes a mapping of the sample space Ω onto the target space Γ. Therefore, a random vector $\boldsymbol{\xi} = (\xi_1, \xi_2, \ldots, \xi_{\mathcal{N}}) \in \Gamma$ denote an arbitrary point in the parametric space.

According to the Doob-Dynkin lemma [86], the solution $u(t,\mathbf{x};\omega)$ can be expressed as $u(t,\mathbf{x};\boldsymbol{\xi})$, which provides a very useful tool to work in the target space rather than the abstract

sample space. Thus, the formulation of SFPDE Eqn. (8) can be posed as: Find $u(t,\mathbf{x};\boldsymbol{\xi}) : \mathbb{D}\times\Gamma \to \mathbb{R}$ such that $\forall t,\mathbf{x} \in \mathbb{D}$

$$
\begin{aligned}
&{}_0\mathcal{D}_t^{\alpha(\boldsymbol{\xi})} u(t,\mathbf{x};\boldsymbol{\xi}) - \sum_{j=1}^{d} k_j \left[{}_{a_j}\mathcal{D}_{x_j}^{\beta_j(\boldsymbol{\xi})} + {}_{x_j}\mathcal{D}_{b_j}^{\beta_j(\boldsymbol{\xi})} \right] u(t,\mathbf{x};\boldsymbol{\xi}) \\
&= h(t,\mathbf{x}) + f(t;\boldsymbol{\xi}) \qquad (20)
\end{aligned}
$$

holds ρ-a.s. for $\boldsymbol{\xi}(\omega) \in \Gamma$ and $\forall t,\mathbf{x} \in \mathbb{D}$, subject to proper initial and boundary conditions.

3.4 Stochastic Sampling

We expound the two sampling methods, MCS and PCM to sample from random space and, then propagate the associated uncertainties by computing the statistics of stochastic solutions via post processing.

Monte Carlo Sampling: MCS. The general procedure in statistical Monte Carlo sampling is the three following steps.

1. Generating a set of random variables $\boldsymbol{\xi}_i$, $i = 1,2,\cdots,K$ for a prescribed number of realizations K.
2. Solving the deterministic problem Eqn. (20) and obtaining the solution $u_i = u(t,\mathbf{x};\boldsymbol{\xi}_i)$ for each $i = 1,2,\cdots,K$.
3. Computing the solution statistics, e.g. $\mathbb{E}[u] = \frac{1}{M}\sum_{i=1}^{M} u_i$.

We note that step 1 and 3 are pre- and post- processing steps, respectively. Step 2 requires repetitive simulation of deterministic counterpart of the problem, which we obtain by developing a Petrov-Galerkin spectral method in the physical domain. Although MCS is relatively easy to implement once a deterministic forward solver is developed, it requires too many samplings for the solution statistics to converge, and yet the extra numerical cost due to non-locality and memory effect in fractional operators are still remained. In addition, the number of required sampling also grows rapidly as the dimension of problem increases, resulting in an exhaustively long run time for the statistics to converge.

Probability Collocation Method: PCM. We employ a high-order stochastic discretization in the random space following [37, 87] in order to construct a probabilistic collocation method (PCM), which yields a high convergence rate with much fewer number of sampling. The idea of PCM is based on polynomial interpolation, however in the random space. Let $\Theta_{\mathcal{N}} = \{\xi_i\}_{i=1}^{\mathcal{J}}$ be a set of prescribed sampling points. By employing the Lagrange interpolation polynomials L_i, the polynomial approximation $\mathcal{I}$ of the stochastic solution u in the random space can be expressed as:

$$
\hat{u}(t,\mathbf{x};\boldsymbol{\xi}) = \mathcal{I}u(t,\mathbf{x};\boldsymbol{\xi}) = \sum_{i=1}^{\mathcal{J}} u(t,\mathbf{x};\xi_i) L_i(\boldsymbol{\xi}). \qquad (21)
$$

Therefore, the collocation procedure of solving Eqn. (20) to obtain the stochastic solution u is:

$$
R(\hat{u}(t,\mathbf{x};\boldsymbol{\xi}))\Big|_{\xi_i} = \left(\mathcal{L}^{q(\boldsymbol{\xi})}\hat{u}(t,\mathbf{x};\boldsymbol{\xi})) - F(t,\mathbf{x};\boldsymbol{\xi}) \right)\Big|_{\xi_i} = 0, \qquad (22)
$$

for $i = 1,2,\cdots,\mathcal{J}$, where $\mathcal{L}^q$ is given in Eqn. (11). By using the property of Lagrange interpolants that satisfy the Kronecker delta at the interpolation points, we obtain:

$$
\mathcal{L}^{q(\xi_i)} u(t,\mathbf{x};\xi_i)) = F(t,\mathbf{x};\xi_i), \quad i = 1,2,\cdots,\mathcal{J}, \qquad (23)
$$

subject to proper initial/boundary conditions. Thus, the probabilistic collocation procedure is equivalent to solving $\mathcal{J}$ deterministic problems Eqn. (23) with conditions Eqn. (9) and Eqn. (10). Once the deterministic solutions are obtained at each sampling point, the numerical stochastic solution is interpolated, using Eqn. (21) to construct a global approximate $\hat{u}(t,\mathbf{x};\boldsymbol{\xi})$. We then obtain the solution statistics as

$$
\mathbb{E}[\hat{u}] = \int_{\Gamma} \hat{u}(t,\mathbf{x};\boldsymbol{\xi})\rho(\boldsymbol{\xi})\,\mathrm{d}\boldsymbol{\xi}, \ \sigma[u] = \sqrt{\mathbb{E}[\hat{u}^2] - \mathbb{E}[\hat{u}]^2}. \qquad (24)
$$

The above integrals can be computed efficiently by letting the interpolation/collocation points to be the same as a set of cubature rules $\Theta_{\mathcal{N}} = \{\xi_i\}_{i=1}^{\mathcal{J}}$ on the parametric space with integration weights $\{\mathbf{w}_i\}_{i=1}^{\mathcal{J}}$, which are employed in computing the integral. By property of Kronecker delta of Lagrange interpolant and use of any quadrature rule over the above integral yields

$$
\mathbb{E}[\hat{u}(t,\mathbf{x}:\boldsymbol{\xi})] \approx \sum_{i=1}^{\mathcal{J}} w_i\, u(t,\mathbf{x};\xi_i). \qquad (25)
$$

Choice of Collocation/Interpolation Points. A natural choice of the sampling points is the tensor-product of one-dimensional sets, which is efficients for low-dimensional random spaces. However, in high-dimensional multivariate case, where $\mathcal{N} > 6$, the tensor-product interpolation operators are computationally expensive due to the increasing nested summation loops. In addition, the total number of sampling points grows rapidly by increase of dimension by $\mathcal{J}^{\mathcal{N}}$, where $\mathcal{J}$ is the number of points in each direction.

Another choice that provides an alternative to the more costly full tensor product rule is the isotropic Smolyak sparse grid operator $A(w,\mathcal{N})$ [39, 40] with two input parameters dimension size $\mathcal{N}$ and the level of grid w. The Smolyak algorithm significantly reduces the total number of sampling points; see Fig. 1 for comparison of $A(2,2)$, $A(4,2)$, and $A(6,2)$ with full tensor product rule for a two-dimensional random spaces. The total number of sampling points for each case is also listed in Tab.1. More research has also been devoted to the analysis and construction of Smolyak sparse grids [37, 88–90].

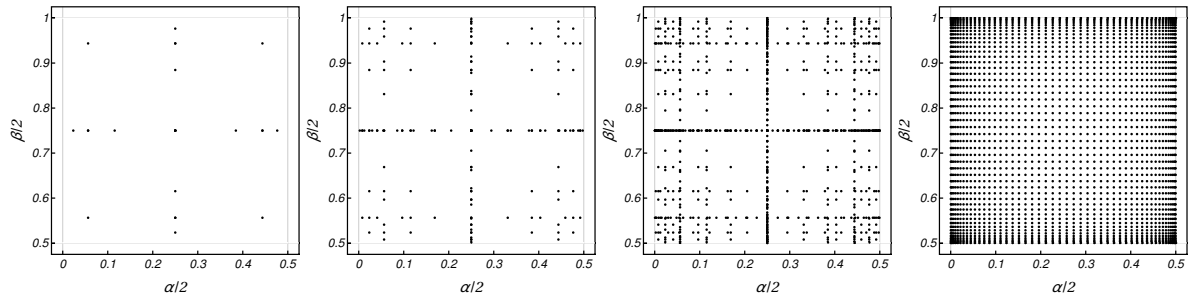

Fig. 1: Illustration of sampling nodal points in two-dimensional random space, using Smolyak sparse grid generator (a) $A(2,2)$, (b) $A(4,2)$,(c) $A(6,2)$; and (d) full tensor product rule with 50 points in each direction. The total number of points in each case is, 25, 161, 837, and 2500, respectively.

Space dimensionality	Full tensor product	Smolyak sparse grid generator $A(w,\mathcal{N})$				
$\mathcal{N}$		$w=2$	$w=4$	$w=6$	$w=8$	$w=10$
2	10^2	25	161	837	4105	19469
5	10^5	131	3376	45458	440953	3542465
15	10^{15}	1066	197176	15480304		
25	10^{25}	2901	1445975			
55	10^{55}	87780				

Table 1: The total number of nodal points in random space sampling, using Smolyak sparse grid generator and full tensor product with 10 points in each direction.

4 Forward Solver

For each realization of random variables in the employed sampling methods, the stochastic model yields a deterministic FPDE, left to be solved in the physical domain. We recall that for every $\boldsymbol{\xi}_i, i = 1,2,\cdots$ in SFPDE Eqn. (20), the deterministic problem is recast as:

$$ {}_0\mathcal{D}_t^{\alpha} u(t,\mathbf{x}) - \sum_{j=1}^{d} k_j \left[{}_{a_j}\mathcal{D}_{x_j}^{\beta_j} + {}_{x_j}\mathcal{D}_{b_j}^{\beta_j} \right] u(t,\mathbf{x}) = h(t,\mathbf{x}) + f(t), \tag{26} $$

subject to the same initial/boundary conditions as Eqn. (9) and Eqn. (10). In the sequel, we develop a Petrov-Galerkin spectral method to numerically solve the deterministic problem in the physical domain. We also show the wellposedness of deterministic problem in a weak sense and further investigate the stability of proposed numerical scheme.

4.1 Mathematical Framework

The comprehensive development of mathematical framework and stability analysis of numerical method are given in Appendix A. Here, we only discuss the essential requirement for the rest of the paper.

We denote the fractional Sobolev space on $\mathbb{R}$ by $H^{\sigma}(\mathbb{R})$, $\sigma \geq 0$, which is endowed with some proper norms. Let $I = [0,T]$, $\Lambda_1 = (a_1,b_1)$, $\Lambda_j = (a_j,b_j) \times \Lambda_{j-1}$ for $j = 2,\cdots,d$. We define $\mathcal{X}_1 = H_0^{\frac{\beta_1}{2}}(\Lambda_1)$, and accordingly, $\mathcal{X}_j$, $j = 2,\cdots,d$ as

$$ \mathcal{X}_2 = H_0^{\frac{\beta_2}{2}}\Big((a_2,b_2);L^2(\Lambda_1)\Big) \cap L^2((a_2,b_2);\mathcal{X}_1), \tag{27} $$

$$ \vdots $$

$$ \mathcal{X}_d = H_0^{\frac{\beta_d}{2}}\Big((a_d,b_d);L^2(\Lambda_{d-1})\Big) \cap L^2((a_d,b_d);\mathcal{X}_{d-1}), \tag{28} $$

and thus, define the "solution space" U and "test space" V as

$$ \begin{aligned} U &= {}_0^l H^{\frac{\alpha}{2}}\Big(I;L^2(\Lambda_d)\Big) \cap L^2(I;\mathcal{X}_d), \\ V &= {}_0^r H^{\frac{\alpha}{2}}\Big(I;L^2(\Lambda_d)\Big) \cap L^2(I;\mathcal{X}_d), \end{aligned} \tag{29} $$

respectively, where

$$ \begin{aligned} &{}_0^l H^{\frac{\alpha}{2}}\Big(I;L^2(\Lambda_d)\Big) = \\ &\qquad \Big\{ u \,\Big|\, \|u(t,\cdot)\|_{L^2(\Lambda_d)} \in H^{\frac{\alpha}{2}}(I), u|_{t=0} = u|_{x=a_j} = u|_{x=b_j} = 0 \Big\}, \\ &{}_0^r H^{\frac{\alpha}{2}}\Big(I;L^2(\Lambda_d)\Big) = \\ &\qquad \Big\{ v \,\Big|\, \|v(t,\cdot)\|_{L^2(\Lambda_d)} \in H^{\frac{\alpha}{2}}(I), v|_{t=T} = v|_{x=a_j} = v|_{x=b_j} = 0 \Big\}. \end{aligned} $$

For any realization of Eqn. (20), we obtain the weak system, i.e. the variational form of the deterministic counterpart of the problem, subject to the given initial/boundary conditions, by multiplying the equation with proper test functions and integrating over the whole computational domain $\mathbb{D}$. By using Lemmas A.3-A.5, the bilinear form can be written as

$$\begin{aligned} a(u,v) =& ({}_0\mathcal{D}_t^{\frac{\alpha}{2}} u, {}_t\mathcal{D}_T^{\frac{\alpha}{2}} v)_{\mathbb{D}} \\ &- \sum_{j=1}^{d} k_j \Big[({}_{a_j}\mathcal{D}_{x_j}^{\frac{\beta_j}{2}} u, {}_{x_j}\mathcal{D}_{b_j}^{\frac{\beta_j}{2}} v)_{\mathbb{D}} + ({}_{x_j}\mathcal{D}_{b_j}^{\frac{\beta_j}{2}} u, {}_{a_j}\mathcal{D}_{x_j}^{\frac{\beta_j}{2}} v)_{\mathbb{D}} \Big], \end{aligned} \tag{30}$$

and thus, by letting U and V be the proper solution/test spaces, the problem reads as: find $u \in U$ such that

$$a(u,v) = (\mathrm{f}, v)_{\mathbb{D}}, \quad \forall v \in V, \tag{31}$$

where $\mathrm{f} = h(t,\mathbf{x}) + f(t)$.

4.2 Petrov-Galerkin Spectral Method

We define the following finite dimensional solution and test spaces. We first denote the Jacobi polynomials of order n with parameters A, B by $P_n^{A,B}(x)$, where $A = B = 0$ gives the Legendre polynomial $P_n(x)$ of order n. We also denote the Jacobi poly-fractonomial of first kind with parameter τ by ${}^{(1)}\mathcal{P}_n^{\tau}(x) = (1+x)^{\tau} P_{n-1}^{-\tau,\tau}(x)$. Thus, we employ Legendre polynomials $\phi_{m_j}(\xi)$, $j = 1,2,\cdots,d$, and Jacobi poly-fractonomial of first kind $\psi_n^{\tau}(\eta)$ [59,60], as the spatial and temporal bases, respectively, given in their corresponding standard domain as

$$\phi_{m_j}(\xi) = \sigma_{m_j}(P_{m_j+1}(\xi) - P_{m_j-1}(\xi)), \tag{32}$$

$$\psi_n^{\tau}(\eta) = \sigma_n \, {}^{(1)}\mathcal{P}_n^{\tau}(\eta) = \sigma_n (1+\eta)^{\tau} P_{n-1}^{-\tau,\tau}(\eta), \tag{33}$$

in which $\xi \in [-1,1]$, $m_j = 1,2,\cdots$, $\sigma_{m_j} = 2 + (-1)^{m_j}$, $\eta \in [-1,1]$, $n = 1,2,\cdots$, and $\sigma_n = 2 + (-1)^n$. Therefore, by performing affine mappings $\eta = 2\frac{t}{T} - 1$ and $\xi = 2\frac{x-a_j}{b_j-a_j} - 1$ from the computational domain to the standard domain, we construct the solution space U_N as

$$\begin{aligned} U_N = span\Big\{ \big(\psi_n^{\tau} \circ \eta\big)(t) \prod_{j=1}^{d} \big(\phi_{m_j} \circ \xi\big)(x_j) \\ : n = 1,2,\cdots,\mathcal{N},\ m_j = 1,2,\cdots,\mathcal{M}_j \Big\}. \end{aligned} \tag{34}$$

We note that the choice of temporal and spatial basis functions naturally satisfy the initial and boundary conditions, respectively. The parameter τ in the temporal basis functions plays a role of fine tunning parameter, which can be chosen properly to capture the singularity of exact solution.

Moreover, we employ Legendre polynomials $\Phi_{r_j}(\xi)$, $j = 1,2,\cdots,d$, and Jacobi poly-fractonomial of second kind $\Psi_k^{\tau}(\eta)$, as the spatial and temporal test functions, respectively, given in their corresponding standard domain as

$$\Phi_{r_j}(\xi) = \widetilde{\sigma}_{r_j}(P_{r_j+1}(\xi) - P_{r_j-1}(\xi)), \tag{35}$$

$$\Psi_k^{\tau}(\eta) = \widetilde{\sigma}_k \, {}^{(2)}\mathcal{P}_k^{\tau}(\eta) = \widetilde{\sigma}_k (1-\eta)^{\tau} P_{k-1}^{\tau,-\tau}(\eta), \tag{36}$$

where $\xi \in [-1,1]$, $r_j = 1,2,\cdots$, $\widetilde{\sigma}_{r_j} = 2(-1)^{r_j} + 1$, $\eta \in [-1,1]$, $k = 1,2,\cdots$, and $\widetilde{\sigma}_k = 2(-1)^k + 1$. Therefore, by similar affine mapping we construct the test space V_N as

$$\begin{aligned} V_N = span\Big\{ \big(\Psi_k^{\tau} \circ \eta\big)(t) \prod_{j=1}^{d} \big(\Phi_{r_j} \circ \xi_j\big)(x_j) \\ : k = 1,2,\cdots,\mathcal{N},\ r_j = 1,2,\cdots,\mathcal{M}_j \Big\}. \end{aligned} \tag{37}$$

Thus, since $U_N \subset U$ and $V_N \subset V$, the problems Eqn. (31) read as: find $u_N \in U_N$ such that

$$a_h(u_N, v_N) = l(v_N), \quad \forall v_N \in V_N, \tag{38}$$

where $l(v_N) = (\mathrm{f}, v_N)$. The discrete bilinear form $a_h(u_N, v_N)$ can be written as

$$\begin{aligned} a_h(u_N, v_N) =& ({}_0\mathcal{D}_t^{\frac{\alpha}{2}} u_N, {}_t\mathcal{D}_T^{\frac{\alpha}{2}} v_N)_{\mathbb{D}} \\ &- \sum_{j=1}^{d} k_j \Big[({}_{a_j}\mathcal{D}_{x_j}^{\frac{\beta_j}{2}} u_N, {}_{x_j}\mathcal{D}_{b_j}^{\frac{\beta_j}{2}} v_N)_{\mathbb{D}} + ({}_{x_j}\mathcal{D}_{b_j}^{\frac{\beta_j}{2}} u_N, {}_{a_j}\mathcal{D}_{x_j}^{\frac{\beta_j}{2}} v_N)_{\mathbb{D}} \Big]. \end{aligned} \tag{39}$$

We expand the approximate solution $u_N \in U_N$, satisfying the discrete bilinear form Eqn. (39), in the following form

$$\begin{aligned} &u_N(t,\mathbf{x}) = \\ &\sum_{n=1}^{\mathcal{N}} \sum_{m_1=1}^{\mathcal{M}_1} \cdots \sum_{m_d=1}^{\mathcal{M}_d} \hat{u}_{n,m_1,\cdots,m_d} \Big[\big(\psi_n^{\tau} \circ \eta\big)(t) \prod_{j=1}^{d} \big(\phi_{m_j} \circ \xi\big)(x_j) \Big], \end{aligned} \tag{40}$$

and obtain the corresponding Lyapunov system by substituting Eqn. (40) into Eqn. (39) by choosing

$$\begin{aligned} &v_N(t,\mathbf{x}) = \\ &\big(\Psi_k^{\tau} \circ \eta\big)(t) \prod_{j=1}^{d} \big(\Phi_{r_j} \circ \xi_j\big)(x_j),\ k = 1,2,\ldots,\mathcal{N},\ r_j = 1,2,\ldots,\mathcal{M}_j. \end{aligned}$$

Therefore,

$$\begin{aligned} &\Big[S_T \otimes M_1 \otimes M_2 \cdots \otimes M_d \\ &+ \sum_{j=1}^{d} M_T \otimes M_1 \otimes \cdots \otimes M_{j-1} \otimes S_j \otimes M_{j+1} \cdots \otimes M_d \Big] \mathcal{U} = F, \end{aligned} \tag{41}$$

in which $\otimes$ represents the Kronecker product, F denotes the multi-dimensional load matrix whose entries are given as

$$F_{k,r_1,\cdots,r_d} = \int_{\mathbb{D}} \mathrm{f}(t,\mathbf{x})\Big(\Psi_k^{\tau}\circ\eta\Big)(t)\prod_{j=1}^{d}\Big(\Phi_{r_j}\circ\xi_j\Big)(x_j)\,d\mathbb{D}, \quad (42)$$

and $\mathcal{U}$ is the matrix of unknown coefficients. The matrices S_T and M_T denote the temporal stiffness and mass matrices, respectively; and the matrices S_j and M_j denote the spatial stiffness and mass matrices, respectively. We obtain the entries of spatial mass matrix M_j analytically and employ proper quadrature rules to accurately compute the entries of other matrices S_T, M_T and S_j.

We note that the choices of basis/test functions, employed in developing the PG scheme leads to symmetric mass and stiffness matrices, providing useful properties to further develop a fast solver. The following Theorem 4.1 provides a unified fast solver, developed in terms of the generalized eigensolutions in order to obtain a closed-form solution to the Lyapunov system Eqn. (41).

Theorem 4.1 (Unified Fast FPDE Solver [65]). *Let $\{\vec{e}_{m_j},\lambda_{m_j}\}_{m_j=1}^{\mathcal{M}_j}$ be the set of general eigen-solutions of the spatial stiffness matrix S_j with respect to the mass matrix M_j. Moreover, let $\{\vec{e}_n^{\tau},\lambda_n^{\tau}\}_{n=1}^{\mathcal{N}}$ be the set of general eigen-solutions of the temporal mass matrix M_T with respect to the stiffness matrix S_T. Then, the matrix of unknown coefficients $\mathcal{U}$ is explicitly obtained as*

$$\mathcal{U} = \sum_{n=1}^{\mathcal{N}}\sum_{m_1=1}^{\mathcal{M}_1}\cdots\sum_{m_d=1}^{\mathcal{M}_d}\kappa_{n,m_1,\cdots,m_d}\,\vec{e}_n^{\tau}\otimes\vec{e}_{m_1}\otimes\cdots\otimes\vec{e}_{m_d}, \quad (43)$$

where $\kappa_{n,m_1,\cdots,m_d}$ is given by

$$\kappa_{n,m_1,\cdots,m_d} = \frac{(\vec{e}_n^{\tau}\vec{e}_{m_1}\cdots\vec{e}_{m_d})F}{\Big[(\vec{e}_n^{\tau^T}S_T\vec{e}_n^{\tau})\prod_{j=1}^{d}(\vec{e}_{m_j}^{T}M_j\vec{e}_{m_j})\Big]\Lambda_{n,m_1,\cdots,m_d}} \quad (44)$$

in which the numerator represents the standard multi-dimensional inner product, and $\Lambda_{n,m_1,\cdots,m_d}$ is obtained in terms of the eigenvalues of all mass matrices as

$$\Lambda_{n,m_1,\cdots,m_d} = \Big[1+\lambda_n^{\tau}\textstyle\sum_{j=1}^{d}(\lambda_{m_j})\Big].$$

5 Numerical Results

We investigate the performance of developed numerical methods by considering couple of numerical simulations. We compare MCS and PCM in random space discretization while using PG method in physical domain. We note that by several numerical examples, we make sure that the developed PG method is stable and accurate in solving each deterministic problem; the results are not provided here.

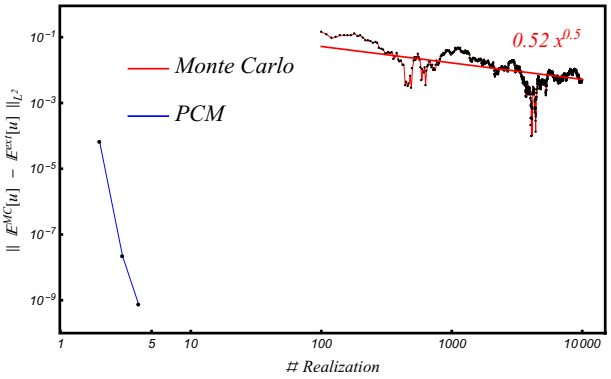

Fig. 2: L^2-norm convergence rate of MCM and PCM for stochastic fractional IVP Eqn. (45).

5.1 Low-Dimensional Random Inputs

As the first case, we consider a stochastic fractional initial value problem (IVP) with random fractional index by letting the diffusion coefficient to be zero, and also ignoring the additional random input and only taking $h(t)$ as the external forcing term. Therefore, we obtain

$${}_0\mathcal{D}_t^{\alpha(\xi)}u(t;\xi) = h(t), \quad (45)$$

subject to zero initial condition, where $u(t,\xi):(0,T]\times\Lambda\to\mathbb{R}$. We let $u^{ext}(t) = \frac{\alpha}{2}\,t^{3+\frac{\alpha}{2}}$, $h(t) = {}_0\mathcal{D}_t^{\alpha(\xi)}u^{ext}(t)$ for each realization of α. In this case, by choosing the tunning parameter τ in the temporal basis function to be $\frac{\alpha}{2}$, we can efficiently employ PG numerical scheme and also obtain the exact expectation by rendering the exact solution to be random with similar distribution as the random fractional index. Fig. 2 shows the L^2-norm convergence rate of MCS and PCM in comparison of solution expectation with $\mathbb{E}^{ext}[u] = \mathbb{E}[u^{ext}]$. The results confirms converges rate of 0.5 for MCS, while in PCM, the statistics of solution converges accurately very fast, using only few numbers of realizations. In this example, by ignoring the additional random input to the system, we take the advantage of having the exact random solution to be available.

As another example, we also consider Eqn. (45) with additional random input, expanded by KL expansion with $M = 4$, as:

$${}_0\mathcal{D}_t^{\alpha(\xi)}u(t;\boldsymbol{\xi}) = h(t) + \sum_{k=1}^{M}a_k\,\sin\left(\frac{2k\pi t}{T}\right)\xi_k, \quad (46)$$

with two cases $h(t) = t^2$ and $h(t) = sin(\pi t)$. Fig. 3 shows the mean value and variance of solution for 10^4 sampling of MCS compared to 625 realizations in PCM.

Moreover, we consider (1+1)-D one-sided SFPDE given in Eqn. (20), where $d = 1$ and the diffusion coefficient is k_l. We ignore the additional random input and consider $h(t,x)$ as

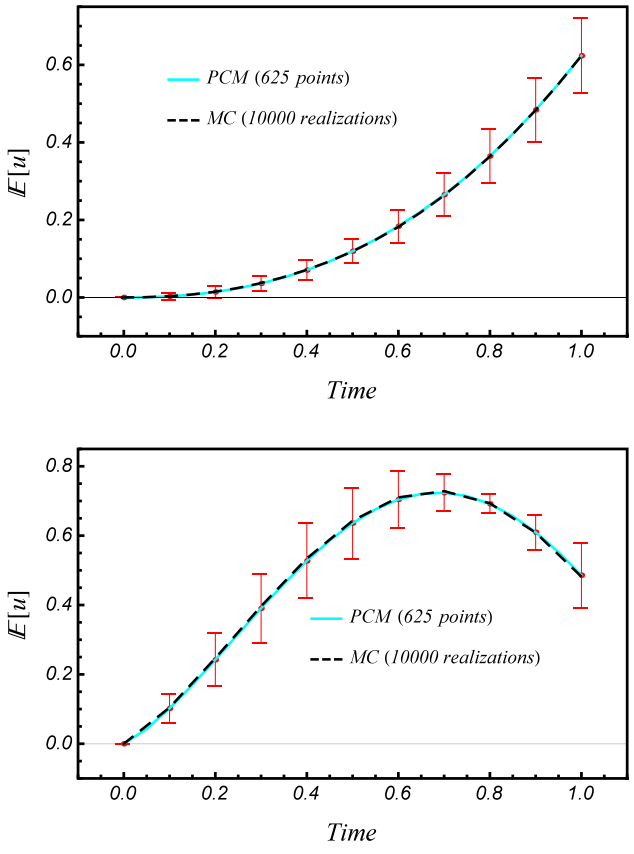

Fig. 3: Expectation of solution to Eqn. (46) with uncertainty (standard deviation) bounds, employing MCS and PCM for (top) $h(t) = t^2$ and (bottom) $h(t) = sin(\pi t)$.

the only external forcing term. Therefore, we obtain

$$ {}_0\mathcal{D}_t^{\alpha(\xi_1)} u(t,x;\boldsymbol{\xi}) - k_{l-1} \mathcal{D}_x^{\beta(\xi_2)} u(t,x;\boldsymbol{\xi}) = h(t,x), \tag{47} $$

subject to zero initial/boundary conditions, where $u(t,x;\boldsymbol{\xi}) : (0,T] \times (-1,1) \times \Lambda \to \mathbb{R}$, and the only random variables are the fractional indices α and β. We let $u^{ext}(t,x) = t^{3+\tau}\left((1+x)^{3+\mu} - \frac{1}{2}(1+x)^{4+\mu}\right)$, and choose $\tau = \alpha/2$ and $\mu = \beta/2$. For each realization of α and β, we obtain the force function $h(t,x)$ by substituting the corresponding u^{ext} to Eqn. (47). Defining $\mathbb{E}^{ext}[u] = \mathbb{E}[u^{ext}]$, Fig. 4 shows the L^2-norm convergence of solution expectation as compared to the exact expectation. We observe that PCM converges accurately with only few number of realizations.

Considering additional random input, expanded by KL expansion with $M = 4$, the problem can be recast as

$$ {}_0\mathcal{D}_t^{\alpha(\boldsymbol{\xi})} u(t,x;\boldsymbol{\xi}) - k_{l-1} \mathcal{D}_x^{\beta(\boldsymbol{\xi})} u(t,x;\boldsymbol{\xi}) = h(t,x) + \sum_{k=1}^{M} a_k \sin\left(\frac{2k\pi t}{T}\right)\xi_k \tag{48} $$

subject to zero initial/boundary conditions. Fig. 5 shows the mean value of solution for MCS and PCM at different times.

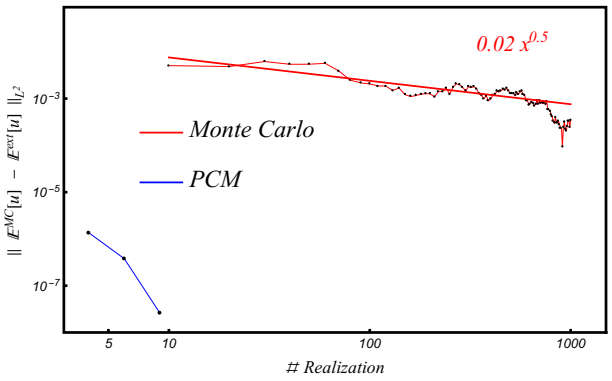

Fig. 4: L^2-norm convergence rate of MCM and PCM for SF-PDE Eqn. (47).

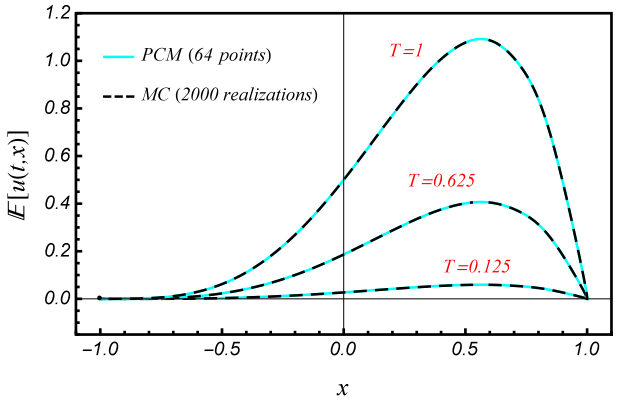

Fig. 5: Expectation of solution to Eqn. (48), employing MCS and PCM at $t = 0.125, 0.625, 1$.

Remark 5.1. *We note that generally use of the sparse grid operators in obtaining solution statistics is more effective when dimension of the random space is higher than 6. Thus, in the numerical examples for low-dimensional random inputs, we employ the easy-to-implement tensor product nodal sets.*

5.2 Moderate- to High-Dimensional Random Inputs

We render the problem with higher number of terms in KL expansion of random inputs in Eqn. (48) by choosing $M = 10$ and $M = 20$. This yields the dimension of random space $\mathcal{N} = 12$ and $\mathcal{N} = 22$, respectively. As mentioned in Remark 5.1, in the case of high-dimensional random space constructing grid based on tensor product rule results in very expensive computation of solution statistics due to exhaustive increase of forward solver instruction. Table 1 shows the comparison between different level of Smolyak algorithm and tensor product rule. Therefore, to obtain the solution statistics, we employ the Smolyak sparse grid generator in the developed PCM. For each cases of KL expansion, we generate the sparse grid on two levels $w = 1$ and $w = 2$, i.e. $A(1,12)$, $A(2,12)$, $A(1,22)$, and $A(2,22)$, where we let the

higher resolution case be a benchmark value to the solution statistics, based on which we compute and normalize the error. We observe that for both cases $N = 12$ and $N = 22$, the normalized error in computing the expectation and standard deviation of solution are of orders $O(10^{-7})$ and $O(10^{-3})$, respectively.

6 Summary and Discussion

We developed a mathematical framework to numerically quantify the solution uncertainty of a stochastic FPDE, associated with the randomness of model parameters. The stochastic FPDE is reformulated by rendering the problem with random fractional indices, subject to additional random noise. We used the truncated Karhunen-Loéve expansion to parametrize the additive noise. Then, by employing a non-intrusive probabilistic collocation method (PCM), we propagated the associated randomness to the system response, by using Smolyak sparse grid generator to construct the set of sample point in the random space. We also formulated a forward solver to simulate the deterministic counterpart of the stochastic problem for each realization of random variables. We showed that the deterministic problem is mathematically well-posed in a weak sense. Furthermore, by employing Jacobi poly-fractonomials and Legendre polynomials as the temporal and spatial basis/test functions, respectively, we developed a Petrove-Galerkin spectral method to solve the deterministic problem in the physical domain. We also proved that the inf-sup condition holds for the proposed numerical scheme, and thus, it is stable. By considering several numerical examples with low- to high-dimensional random spaces, we examined the performance of our stochastic discretization. We showed that in each case, PCM converges very fast to a very high level of accuracy with very few number of sampling.

Acknowledgements

This work was supported by the ARO Young Investigator Program Award (W911NF-19-1-0444), and the National Science Foundation Award (DMS-1923201), also partially by MURI/ARO (W911NF-15-1-0562) and the AFOSR Young Investigator Program Award (FA9550-17-1-0150).

A Mathematical Framework of Deterministic Solver

Here, we extensively discuss the mathematical framework of the developed method in details.

A.1 Mathematical Framework

We define the useful functional spaces and their associated norms [52, 69]. By $H^\sigma(\mathbb{R}) = \{u(t) | u \in L^2(\mathbb{R}); (1+|\omega|^2)^{\frac{\sigma}{2}}\mathcal{F}(u)(\omega) \in L^2(\mathbb{R})\}$, $\sigma \geq 0$, we denote the fractional Sobolev space on $\mathbb{R}$, endowed with norm $\|u\|_{H^\sigma_{\mathbb{R}}} = \|(1+|\omega|^2)^{\frac{\sigma}{2}}\mathcal{F}(u)(\omega)\|_{L^2(\mathbb{R})}$, where $\mathcal{F}(u)$ represents the Fourier transform of u. Subsequently, we denote by $H^\sigma(\Lambda) = \{u \in L^2(\Lambda) \,|\, \exists \tilde{u} \in H^\sigma(\mathbb{R}) \; s.t. \; \tilde{u}|_\Lambda = u\}$, $\sigma \geq 0$, the fractional Sobolev space on any finite closed interval, e.g. $\Lambda = (a,b)$, with norm $\|u\|_{H^\sigma(\Lambda)} = \inf_{\tilde{u} \in H^\sigma_{\mathbb{R}}, \tilde{u}|_\Lambda = u} \|\tilde{u}\|_{H^\sigma(\mathbb{R})}$. We define the following useful norms as:

$$
\begin{aligned}
\|\cdot\|_{{}^lH^\sigma(\Lambda)} &= \left(\|{}_a\mathcal{D}_x^\sigma(\cdot)\|^2_{L^2(\Lambda)} + \|\cdot\|^2_{L^2(\Lambda)}\right)^{\frac{1}{2}}, \\
\|\cdot\|_{{}^rH^\sigma(\Lambda)} &= \left(\|{}_x\mathcal{D}_b^\sigma(\cdot)\|^2_{L^2(\Lambda)} + \|\cdot\|^2_{L^2(\Lambda)}\right)^{\frac{1}{2}}, \\
\|\cdot\|_{{}^cH^\sigma(\Lambda)} &= \left(\|{}_x\mathcal{D}_b^\sigma(\cdot)\|^2_{L^2(\Lambda)} + \|{}_a\mathcal{D}_x^\sigma(\cdot)\|^2_{L^2(\Lambda)} + \|\cdot\|^2_{L^2(\Lambda)}\right)^{\frac{1}{2}},
\end{aligned}
$$

where the equivalence of $\|\cdot\|_{{}^lH^\sigma(\Lambda)}$ and $\|\cdot\|_{{}^rH^\sigma(\Lambda)}$ are shown in [52, 53, 91].

Lemma A.1. *Let $\sigma \geq 0$ and $\sigma \neq n - \frac{1}{2}$. Then, the norms $\|\cdot\|_{{}^lH^\sigma(\Lambda)}$ and $\|\cdot\|_{{}^rH^\sigma(\Lambda)}$ are equivalent to $\|\cdot\|_{{}^cH^\sigma(\Lambda)}$.*

We also define $C_0^\infty(\Lambda)$ as the space of smooth functions with compact support in (a,b). We denote by ${}^lH_0^\sigma(\Lambda)$, ${}^rH_0^\sigma(\Lambda)$, and ${}^cH_0^\sigma(\Lambda)$ as the closure of $C_0^\infty(\Lambda)$ with respect to the norms $\|\cdot\|_{{}^lH^\sigma(\Lambda)}$, $\|\cdot\|_{{}^rH^\sigma(\Lambda)}$, and $\|\cdot\|_{{}^cH^\sigma(\Lambda)}$. It is shown in [53, 91] that these Sobolev spaces are equal and their seminorms are also equivalent to $|\cdot|^*_{H^\sigma(\Lambda)} = \left|\left({}_a\mathcal{D}_x^\sigma(\cdot), {}_x\mathcal{D}_b^\sigma(\cdot)\right)\right|^{\frac{1}{2}}_\Lambda$. Therefore, we can prove that $\left|({}_a\mathcal{D}_x^\sigma u, {}_x\mathcal{D}_b^\sigma v)_\Lambda\right| \geq \beta |u|_{{}^lH^\sigma(\Lambda)} |v|_{{}^rH^\sigma(\Lambda)}$ and $\left|({}_x\mathcal{D}_b^\sigma u, {}_a\mathcal{D}_x^\sigma v)_\Lambda\right| \geq \beta |u|_{{}^rH^\sigma(\Lambda)} |v|_{{}^lH^\sigma(\Lambda)}$, in which β is a positive constant.

Moreover, by letting ${}_0C^\infty(I)$ and $C_0^\infty(I)$ be the space of smooth functions with compact support in $(0,T]$ and $[0,T)$, respectively, we define ${}^lH^s(I)$ and ${}^rH^s(I)$ as the closure of ${}_0C^\infty(I)$ and $C_0^\infty(I)$ with respect to the norms $\|\cdot\|_{{}^lH^s(I)}$ and $\|\cdot\|_{{}^rH^s(I)}$. Other equivalent useful semi-norms associated with $H^s(I)$ are also introduced in [52, 91], as $|\cdot|_{{}^lH^s(I)} = \|{}_0\mathcal{D}_t^s(\cdot)\|_{L^2(I)}$, $|\cdot|_{{}^rH^s(I)} = \|{}_t\mathcal{D}_T^s(\cdot)\|_{L^2(I)}$, $|\cdot|^*_{H^s(I)} = \left|\left({}_0\mathcal{D}_t^s(\cdot), {}_t\mathcal{D}_T^s(\cdot)\right)_I\right|^{\frac{1}{2}}$, where $|\cdot|^*_{H^s(I)} \equiv |\cdot|^{\frac{1}{2}}_{{}^lH^s(I)} |\cdot|^{\frac{1}{2}}_{{}^rH^s(I)}$.

Borrowing definitions from [65], we define the following spaces, which we use later in construction of corresponding solution and test spaces of our problem. Thus, by letting $\Lambda_1 = (a_1, b_1)$, $\Lambda_j = (a_j, b_j) \times \Lambda_{j-1}$ for $j = 2, \cdots, d$, we define $\mathcal{X}_1 = H_0^{\frac{\beta_1}{2}}(\Lambda_1)$, which is associated with the norm $\|\cdot\|_{{}^cH^{\frac{\beta_1}{2}}(\Lambda_1)}$, and accordingly, $\mathcal{X}_j$, $j = 2, \cdots, d$ as

$$
\mathcal{X}_2 = H_0^{\frac{\beta_2}{2}}\Big((a_2,b_2); L^2(\Lambda_1)\Big) \cap L^2((a_2,b_2); \mathcal{X}_1), \tag{49}
$$

$$
\vdots
$$

$$
\mathcal{X}_d = H_0^{\frac{\beta_d}{2}}\Big((a_d,b_d); L^2(\Lambda_{d-1})\Big) \cap L^2((a_d,b_d); \mathcal{X}_{d-1}), \tag{50}
$$

associated with norms

$$
\|\cdot\|_{\mathcal{X}_j} = \left\{\|\cdot\|^2_{H_0^{\frac{\beta_j}{2}}\left((a_j,b_j); L^2(\Lambda_{j-1})\right)} + \|\cdot\|^2_{L^2\left((a_j,b_j); \mathcal{X}_{j-1}\right)}\right\}^{\frac{1}{2}},
$$

for $j = 2, 3, \cdots, d$.

Lemma A.2. *Let $\beta_j \geq 0$ and $\beta_j \neq n - \frac{1}{2}$. Then, for $j = 1, 2, \cdots, d$*

$$
\|\cdot\|_{\mathcal{X}_j} \equiv \left\{\sum_{i=1}^{j}\left(\|{}_{x_i}\mathcal{D}_{b_i}^{\beta_i/2}(\cdot)\|^2_{L^2(\Lambda_j)} + \|{}_{a_i}\mathcal{D}_{x_i}^{\beta_i/2}(\cdot)\|^2_{L^2(\Lambda_j)}\right) + \|\cdot\|^2_{L^2(\Lambda_j)}\right\}^{\frac{1}{2}}.
$$

Solution and Test Spaces

We define the "solution space" U and "test space" V, respectively, as

$$
\begin{aligned}
U &= {}_0^lH^{\frac{\alpha}{2}}\Big(I; L^2(\Lambda_d)\Big) \cap L^2(I; \mathcal{X}_d), \\
V &= {}_0^rH^{\frac{\alpha}{2}}\Big(I; L^2(\Lambda_d)\Big) \cap L^2(I; \mathcal{X}_d),
\end{aligned}
$$

endowed with norms

$$
\begin{aligned}
\|u\|_U &= \left\{\|u\|^2_{{}^lH^{\frac{\alpha}{2}}(I; L^2(\Lambda_d))} + \|u\|^2_{L^2(I;\mathcal{X}_d)}\right\}^{\frac{1}{2}}, \\
\|v\|_V &= \left\{\|v\|^2_{{}^rH^{\frac{\alpha}{2}}(I; L^2(\Lambda_d))} + \|v\|^2_{L^2(I;\mathcal{X}_d)}\right\}^{\frac{1}{2}},
\end{aligned} \tag{51}
$$

where $I = [0,T]$, and

$$
\begin{aligned}
&{}_0^lH^{\frac{\alpha}{2}}\Big(I; L^2(\Lambda_d)\Big) = \\
&\qquad \Big\{u \,\Big|\, \|u(t,\cdot)\|_{L^2(\Lambda_d)} \in H^{\frac{\alpha}{2}}(I), u|_{t=0} = u|_{x=a_j} = u|_{x=b_j} = 0\Big\}, \\
&{}_0^rH^{\frac{\alpha}{2}}\Big(I; L^2(\Lambda_d)\Big) = \\
&\qquad \Big\{v \,\Big|\, \|v(t,\cdot)\|_{L^2(\Lambda_d)} \in H^{\frac{\alpha}{2}}(I), v|_{t=T} = v|_{x=a_j} = v|_{x=b_j} = 0\Big\},
\end{aligned}
$$

equipped with norms $\|u\|_{{}^lH^{\frac{\alpha}{2}}(I; L^2(\Lambda_d))}$ and $\|u\|_{{}^rH^{\frac{\alpha}{2}}(I; L^2(\Lambda_d))}$, respectively. We can show that these norms take the following

forms

$$\begin{aligned}\|u\|_{{}_lH^{\frac{\alpha}{2}}(I;L^2(\Lambda_d))} &= \Big\| \|u(t,\cdot)\|_{L^2(\Lambda_d)} \Big\|_{{}_lH^{\frac{\alpha}{2}}(I)} \\ &= \Big(\|{}_0\mathcal{D}_t^{\frac{\alpha}{2}}(u)\|^2_{L^2(\Omega)} + \|u\|^2_{L^2(\Omega)} \Big)^{\frac{1}{2}}, \\ \|u\|_{{}_rH^{\frac{\alpha}{2}}(I;L^2(\Lambda_d))} &= \Big\| \|u(t,\cdot)\|_{L^2(\Lambda_d)} \Big\|_{{}_rH^{\frac{\alpha}{2}}(I)} \\ &= \Big(\|{}_t\mathcal{D}_T^{\frac{\alpha}{2}}(u)\|^2_{L^2(\Omega)} + \|u\|^2_{L^2(\Omega)} \Big)^{\frac{1}{2}}. \end{aligned} \tag{52}$$

Also, using Lemma A.2, we can show that

$$\begin{aligned}\|u\|_{L^2(I;\mathcal{X}_d)} &= \Big\| \|u(t,.)\|_{\mathcal{X}_d} \Big\|_{L^2(I)} \\ &= \Big\{ \|u\|^2_{L^2(\Omega)} + \sum_{j=1}^{d} \big(\|{}_{x_j}\mathcal{D}_{b_j}^{\frac{\beta_j}{2}}(u)\|^2_{L^2(\Omega)} + \|{}_{a_j}\mathcal{D}_{x_j}^{\frac{\beta_j}{2}}(u)\|^2_{L^2(\Omega)} \big) \Big\}^{\frac{1}{2}}. \end{aligned} \tag{53}$$

Therefore, Eqn. (51) can be written as

$$\begin{aligned}\|u\|_U = \Big\{ &\|u\|^2_{L^2(\Omega)} + \|{}_0\mathcal{D}_t^{\frac{\alpha}{2}}(u)\|^2_{L^2(\Omega)} \\ &+ \sum_{j=1}^{d} \big(\|{}_{x_j}\mathcal{D}_{b_j}^{\frac{\beta_j}{2}}(u)\|^2_{L^2(\Omega)} + \|{}_{a_j}\mathcal{D}_{x_j}^{\frac{\beta_j}{2}}(u)\|^2_{L^2(\Omega)} \big) \Big\}^{\frac{1}{2}}, \end{aligned} \tag{54}$$

$$\begin{aligned}\|v\|_V = \Big\{ &\|v\|^2_{L^2(\Omega)} + \|{}_t\mathcal{D}_T^{\frac{\alpha}{2}}(v)\|^2_{L^2(\Omega)} \\ &+ \sum_{j=1}^{d} \big(\|{}_{x_j}\mathcal{D}_{b_j}^{\frac{\beta_j}{2}}(v)\|^2_{L^2(\Omega)} + \|{}_{a_j}\mathcal{D}_{x_j}^{\frac{\beta_j}{2}}(v)\|^2_{L^2(\Omega)} \big) \Big\}^{\frac{1}{2}}. \end{aligned} \tag{55}$$

A.2 Weak Formulation

The following lemmas help us obtain the weak formulation of deterministic problem in the physical domain and construct the numerical scheme.

Lemma A.3. *[52]: For all $\alpha \in (0,1)$, if $u \in H^1([0,T])$ such that $u(0) = 0$, and $v \in H^{\alpha/2}([0,T])$, then $({}_0\mathcal{D}_t^{\alpha}u, v)_\Omega = ({}_0\mathcal{D}_t^{\alpha/2}u, {}_t\mathcal{D}_T^{\alpha/2}v)_\Omega$, where $(\cdot,\cdot)_\Omega$ represents the standard inner product in $\Omega = [0,T]$.*

Lemma A.4. *[69]: Let $1 < \beta < 2$, a and b be arbitrary finite or infinite real numbers. Assume $u \in H^\beta(a,b)$ such that $u(a) = 0$, also ${}_x\mathcal{D}_b^{\beta/2}v$ is integrable in (a,b) such that $v(b) = 0$. Then, $({}_a\mathcal{D}_x^{\beta}u, v) = ({}_a\mathcal{D}_x^{\beta/2}u, {}_x\mathcal{D}_b^{\beta/2}v)$.*

Lemma A.5. *Let $1 < \beta_j < 2$ for $j = 1,2,\cdots,d$, and $u, v \in \mathcal{X}_d$. Then,*

$$\begin{aligned}({}_{a_j}\mathcal{D}_{x_j}^{\beta_j}u, v)_{\Lambda_d} &= ({}_{a_j}\mathcal{D}_{x_j}^{\frac{\beta_j}{2}}u, {}_{x_j}\mathcal{D}_{b_j}^{\frac{\beta_j}{2}}v)_{\Lambda_d}, \\ ({}_{x_j}\mathcal{D}_{b_j}^{\beta_j}u, v)_{\Lambda_d} &= ({}_{x_j}\mathcal{D}_{b_j}^{\frac{\beta_j}{2}}u, {}_{a_j}\mathcal{D}_{x_j}^{\frac{\beta_j}{2}}v)_{\Lambda_d}. \end{aligned}$$

For any realization of Eqn. (20), we obtain the weak system, i.e. the variational form of the deterministic counterpart of the problem, subject to the given initial/boundary conditions, by multiplying the equation with proper test functions and integrate over the whole computational domain $\mathbb{D}$. Using Lemmas A.3-A.5, the bilinear form can be written as

$$\begin{aligned}a(u,v) =& ({}_0\mathcal{D}_t^{\frac{\alpha}{2}}u, {}_t\mathcal{D}_T^{\frac{\alpha}{2}}v)_{\mathbb{D}} \\ &- \sum_{j=1}^{d} k_j \Big[({}_{a_j}\mathcal{D}_{x_j}^{\frac{\beta_j}{2}}u, {}_{x_j}\mathcal{D}_{b_j}^{\frac{\beta_j}{2}}v)_{\mathbb{D}} + ({}_{x_j}\mathcal{D}_{b_j}^{\frac{\beta_j}{2}}u, {}_{a_j}\mathcal{D}_{x_j}^{\frac{\beta_j}{2}}v)_{\mathbb{D}} \Big], \end{aligned} \tag{56}$$

and thus, by letting U and V be the proper solution/test spaces, the problem reads as: find $u \in U$ such that

$$a(u,v) = (\mathrm{f}, v)_{\mathbb{D}}, \quad \forall v \in V, \tag{57}$$

where $\mathrm{f} = h(t,\mathbf{x}) + f(t)$.

A.3 Stability Analysis

We show the well-posedness of deterministic problem and prove the stability of proposed PG scheme.

Lemma A.6. *Let $\alpha \in (0,1)$, $\Omega = I \times \Lambda_d$, and $u \in {}_0^lH^{\alpha/2}(I;L^2(\Lambda_d))$. Then,*

$$\begin{aligned}&\Big| \Big({}_0\mathcal{D}_t^{\alpha/2}u, {}_t\mathcal{D}_T^{\alpha/2}v \Big)_\Omega \Big| \\ &\equiv \|u\|_{{}_lH^{\alpha/2}(I;L^2(\Lambda_d))} \|v\|_{{}_rH^{\alpha/2}(I;L^2(\Lambda_d))}, \quad \forall v \in {}_0^rH^{\alpha/2}(I;L^2(\Lambda_d)). \end{aligned}$$

Moreover,

$$\begin{aligned}&|({}_{a_d}\mathcal{D}_{x_d}^{\beta_d/2}u, {}_{x_d}\mathcal{D}_{b_d}^{\beta_d/2}v)_{\Lambda_d}| \\ &\equiv |u|_{{}_cH^{\beta_d/2}\left((a_d,b_d);L^2(\Lambda_{d-1})\right)} |v|_{{}_cH^{\beta_d/2}\left((a_d,b_d);L^2(\Lambda_{d-1})\right)}, \end{aligned} \tag{58}$$

and

$$\begin{aligned}&|({}_{x_d}\mathcal{D}_{b_d}^{\beta_d/2}u, {}_{a_d}\mathcal{D}_{x_d}^{\beta_d/2}v)_{\Lambda_d}| \\ &\equiv |u|_{{}_cH^{\beta_d/2}\left((a_d,b_d);L^2(\Lambda_{d-1})\right)} |v|_{{}_cH^{\beta_d/2}\left((a_d,b_d);L^2(\Lambda_{d-1})\right)}. \end{aligned} \tag{59}$$

Lemma A.7 (Continuity). *The bilinear form Eqn. (56) is continuous, i.e.,*

$$\forall u \in U,\ \exists \gamma > 0, \quad s.t. \quad |a(u,v)| \le \gamma \|u\|_U \|v\|_V, \quad \forall v \in V. \tag{60}$$

Proof. The proof directly concludes from Eqn. (58) and Lemma A.6.

Theorem A.8 (Stability). *The following inf-sup condition holds for the bilinear form Eqn. (56), i.e.,*

$$\inf_{u \neq 0 \in U} \sup_{v \neq 0 \in V} \frac{|a(u,v)|}{\|v\|_V \|u\|_U} \ge \gamma > 0, \tag{61}$$

where $\Omega = I \times \Lambda_d$ and $\sup_{u \in U} |a(u,v)| > 0$.

Theorem A.9 (well-posedness). *For all* $0 < \alpha < 1$ *and* $1 < \beta_j < 2$*, and* $j = 1, \cdots, d$*, there exists a unique solution to Eqn.* (57)*, continuously dependent on* f*, where* f *belongs to the dual space of* U*.*

Proof. Lemmas A.7 (continuity) and A.8 (stability) yield the well-posedness of weak form Eqn. (57) in (1+d)-dimension due to the generalized Babuška-Lax-Milgram theorem.

Since the defined basis and test spaces are Hilbert spaces, and $U_N \subset U$ and $V_N \subset V$, we can prove that the developed Petrov-Gelerkin spectral method is stable and the following condition holds

$$\inf_{u_N \neq 0 \in U_N} \sup_{v \neq 0 \in V_N} \frac{|a(u_N, v_N)|}{\|v_N\|_V \, \|u_N\|_U} \geq \gamma > 0, \tag{62}$$

with $\gamma > 0$ and independent of N, where $\sup_{u_N \in U_N} |a(u_N, v_N)| > 0$.

References

[1] Zhang, Y., Sun, H., Stowell, H. H., Zayernouri, M., and Hansen, S. E., 2017. "A review of applications of fractional calculus in earth system dynamics". *Chaos, Solitons & Fractals*.

[2] Jaishankar, A., and McKinley, G. H., 2014. "A fractional K-BKZ constitutive formulation for describing the nonlinear rheology of multiscale complex fluids". *Journal of Rheology (1978-present),* **58**(6), pp. 1751–1788.

[3] Jha, R., Kaw, P. K., Kulkarni, D. R., Parikh, J. C., and Team, A., 2003. "Evidence of Lévy stable process in tokamak edge turbulence". *Physics of Plasmas (1994-present),* **10**(3), pp. 699–704.

[4] del Castillo-Negrete, D., Carreras, B. A., and Lynch, V. E., 2004. "Fractional diffusion in plasma turbulence". *Physics of Plasmas (1994-present),* **11**(8), pp. 3854–3864.

[5] Jaishankar, A., and McKinley, G. H., 2013. "Power-law rheology in the bulk and at the interface: quasi-properties and fractional constitutive equations". *Proceedings of the Royal Society A: Mathematical, Physical and Engineering Science,* **469**(2149), p. 20120284.

[6] Naghibolhosseini, M., 2015. "Estimation of outer-middle ear transmission using DPOAEs and fractional-order modeling of human middle ear". PhD thesis, City University of New York, NY.

[7] Naghibolhosseini, M., and Long, G. R., 2017. "Fractional-order modelling and simulation of human ear". *International Journal of Computer Mathematics*, pp. 1–17.

[8] Baeumer, B., Benson, D. A., Meerschaert, M., and Wheatcraft, S. W., 2001. "Subordinated advection-dispersion equation for contaminant transport". *Water Resources Research,* **37**(6), pp. 1543–1550.

[9] Meral, F. C., Royston, T. J., and Magin, R., 2010. "Fractional calculus in viscoelasticity: an experimental study". *Communications in Nonlinear Science and Numerical Simulation,* **15**(4), pp. 939–945.

[10] Cullen, A. C., and Frey, H. C., 1999. *Probabilistic techniques in exposure assessment: a handbook for dealing with variability and uncertainty in models and inputs*. Springer Science & Business Media.

[11] Roy, C. J., and Oberkampf, W. L., 2011. "A comprehensive framework for verification, validation, and uncertainty quantification in scientific computing". *Computer methods in applied mechanics and engineering,* **200**(25), pp. 2131–2144.

[12] Mullins, J., and Mahadevan, S., 2016. "Bayesian uncertainty integration for model calibration, validation, and prediction". *Journal of Verification, Validation and Uncertainty Quantification,* **1**(1), p. 011006.

[13] Der Kiureghian, A., and Ditlevsen, O., 2009. "Aleatory or epistemic? does it matter?". *Structural Safety,* **31**(2), pp. 105–112.

[14] Benson, D. A., Wheatcraft, S. W., and Meerschaert, M. M., 2000. "Application of a fractional advection-dispersion equation". *Water Resources Research,* **36**(6), pp. 1403–1412.

[15] Baeumer, B., Benson, D. A., Meerschaert, M. M., and Wheatcraft, S. W., 2001. "Subordinated advection-dispersion equation for contaminant transport". *Water Resources Research,* **37**(6), pp. 1543–1550.

[16] Fishman, G. S., 1996. Monte carlo: Concepts, algorithms, and applications.

[17] Del Moral, P., Doucet, A., and Jasra, A., 2006. "Sequential monte carlo samplers". *Journal of the Royal Statistical Society: Series B (Statistical Methodology),* **68**(3), pp. 411–436.

[18] Beskos, A., Jasra, A., Law, K., Tempone, R., and Zhou, Y., 2017. "Multilevel sequential monte carlo samplers". *Stochastic Processes and their Applications,* **127**(5), pp. 1417–1440.

[19] Jasra, A., Law, K. J., and Zhou, Y., 2016. "Forward and inverse uncertainty quantification using multilevel monte carlo algorithms for an elliptic nonlocal equation". *International Journal for Uncertainty Quantification,* **6**(6).

[20] Owen, N. E., Challenor, P., Menon, P. P., and Bennani, S., 2017. "Comparison of surrogate-based uncertainty quantification methods for computationally expensive simulators". *SIAM/ASA Journal on Uncertainty Quantification,* **5**(1), pp. 403–435.

[21] Ghanem, R. G., and Spanos, P. D., 2003. *Stochastic finite elements: a spectral approach*. Courier Corporation.

[22] Xiu, D., and Karniadakis, G. E., 2002. "Modeling uncertainty in steady state diffusion problems via generalized polynomial chaos". *Computer methods in applied mechanics and engineering,* **191**(43), pp. 4927–4948.

[23] Xiu, D., and Karniadakis, G. E., 2002. "The Wiener–Askey polynomial chaos for stochastic differential equations". *SIAM journal on scientific computing,* **24**(2), pp. 619–644.

[24] Knio, O. M., and Le Maitre, O. P., 2006. "Uncertainty propagation in cfd using polynomial chaos decomposition". *Fluid Dynamics Research,* **38**(9), pp. 616–640.

[25] Najm, H. N., 2009. "Uncertainty quantification and polynomial chaos techniques in computational fluid dynamics". *Annual review of fluid mechanics,* **41**, pp. 35–52.

[26] Van Dam, N., and Rutland, C., 2016. "Uncertainty quantification of large-eddy spray simulations". *Journal of Verification, Validation and Uncertainty Quantification,* **1**(2), p. 021006.

[27] Babuska, I., Tempone, R., and Zouraris, G. E., 2004. "Galerkin finite element approximations of stochastic elliptic partial differential equations". *SIAM Journal on Numerical Analysis,* **42**(2), pp. 800–825.

[28] Babuška, I., Tempone, R., and Zouraris, G. E., 2005. "Solving elliptic boundary value problems with uncertain coefficients by the finite element method: the stochastic formulation". *Computer methods in applied mechanics and engineering,* **194**(12), pp. 1251–1294.

[29] Le Maıtre, O. P., Knio, O. M. a nd Najm, H. N., and Ghanem, R. G., 2004. "Uncertainty propagation using

Wiener–Haar expansions". *Journal of computational Physics,* **197**(1), pp. 28–57.

[30] Le Maıtre, O. P., Najm, H. N., Ghanem, R. G., and Knio, O. M., 2004. "Multi-resolution analysis of Wiener-type uncertainty propagation schemes". *Journal of Computational Physics,* **197**(2), pp. 502–531.

[31] Schuss, Z., 1980. "Singular perturbation methods in stochastic differential equations of mathematical physics". *Siam Review,* **22**(2), pp. 119–155.

[32] Babuška, I., and Chatzipantelidis, P., 2002. "On solving elliptic stochastic partial differential equations". *Computer Methods in Applied Mechanics and Engineering,* **191**(37), pp. 4093–4122.

[33] Todor, R. A., 2005. "Sparse perturbation algorithms for elliptic pde's with stochastic data". PhD thesis.

[34] Winter, C. L., and Tartakovsky, D. M., 2002. "Groundwater flow in heterogeneous composite aquifers". *Water Resources Research,* **38**(8).

[35] Liu, W. K., Belytschko, T., and Mani, A., 1986. "Probabilistic finite elements for nonlinear structural dynamics". *Computer Methods in Applied Mechanics and Engineering,* **56**(1), pp. 61–81.

[36] Liu, W. K., Belytschko, T., and Mani, A., 1986. "Random field finite elements". *International journal for numerical methods in engineering,* **23**(10), pp. 1831–1845.

[37] Xiu, D., and Hesthaven, J. S., 2005. "High-order collocation methods for differential equations with random inputs". *SIAM Journal on Scientific Computing,* **27**(3), pp. 1118–1139.

[38] Babuška, I., Nobile, F., and Tempone, R., 2007. "A stochastic collocation method for elliptic partial differential equations with random input data". *SIAM Journal on Numerical Analysis,* **45**(3), pp. 1005–1034.

[39] Nobile, F., Tempone, R., and Webster, C. G., 2008. "A sparse grid stochastic collocation method for partial differential equations with random input data". *SIAM Journal on Numerical Analysis,* **46**(5), pp. 2309–2345.

[40] Smolyak, S., 1963. "Quadrature and interpolation formulas for tensor products of certain classes of functions". *Soviet Math. Dokl.,* **4**, pp. 240–243.

[41] Gorenflo, R., Mainardi, F., Moretti, D., and Paradisi, P., 2002. "Time fractional diffusion: a discrete random walk approach". *Nonlinear Dynamics,* **29**(1-4), pp. 129–143.

[42] Sun, Z., and Wu, X., 2006. "A fully discrete difference scheme for a diffusion-wave system". *Applied Numerical Mathematics,* **56**(2), pp. 193–209.

[43] Lin, Y., and Xu, C., 2007. "Finite difference/spectral approximations for the time-fractional diffusion equation". *Journal of Computational Physics,* **225**(2), pp. 1533–1552.

[44] Wang, H., Wang, K., and Sircar, T., 2010. "A direct $O(N\ log^2 N)$ finite difference method for fractional diffusion equations". *Journal of Computational Physics,* **229**(21), pp. 8095–8104.

[45] Wang, K., and Wang, H., 2011. "A fast characteristic finite difference method for fractional advection–diffusion equations". *Advances in Water Resources,* **34**(7), pp. 810–816.

[46] Cao, J., and Xu, C., 2013. "A high order schema for the numerical solution of the fractional ordinary differential equations". *Journal of Computational Physics,* **238**(1), pp. 154–168.

[47] Zeng, F., Li, C., Liu, F., and Turner, I., 2015. "Numerical algorithms for time-fractional subdiffusion equation with second-order accuracy". *SIAM Journal on Scientific Computing,* **37**(1), pp. A55–A78.

[48] Zayernouri, M., and Matzavinos, A., 2016. "Fractional Adams-Bashforth/Moulton methods: An application to the fractional Keller–Segel chemotaxis system". *Journal of Computational Physics-In Press*.

[49] Rawashdeh, E., 2006. "Numerical solution of fractional integro-differential equations by collocation method". *Applied mathematics and computation,* **176**(1), pp. 1–6.

[50] Khader, M., 2011. "On the numerical solutions for the fractional diffusion equation". *Communications in Nonlinear Science and Numerical Simulation,* **16**(6), pp. 2535–2542.

[51] Khader, M., and Hendy, A., 2012. "The approximate and exact solutions of the fractional-order delay differential equations using legendre pseudospectral method". *International Journal of Pure and Applied Mathematics,* **74**(3), pp. 287–297.

[52] Li, X., and Xu, C., 2009. "A space-time spectral method for the time fractional diffusion equation". *SIAM Journal on Numerical Analysis,* **47**(3), pp. 2108–2131.

[53] Li, X., and Xu, C., 2010. "Existence and uniqueness of the weak solution of the space-time fractional diffusion equation and a spectral method approximation". *Communications in Computational Physics,* **8**(5), p. 1016.

[54] Chen, S., Shen, J., and Wang, L., 2014. "Generalized Jacobi functions and their applications to fractional differential equations". *arXiv preprint arXiv:1407.8303*.

[55] Wang, H., and Zhang, X., 2015. "A high-accuracy preserving spectral Galerkin method for the dirichlet boundary-value problem of variable-coefficient conservative fractional diffusion equations". *Journal of Computational Physics,* **281**, pp. 67–81.

[56] Bhrawy, A. H., Doha, E. H., Baleanu, D., and Ezz-Eldien, S. S., 2015. "A spectral tau algorithm based on Jacobi operational matrix for numerical solution of time fractional diffusion-wave equations". *Journal of Computational Physics,* **293**, pp. 142–156.

[57] Karniadakis, G., and Sherwin, S., 2013. *Spectral/hp element methods for computational fluid dynamics*. Oxford University Press.

[58] Canuto, C., Hussaini, M. Y., Quarteroni, A., and Zang, T. A., 2006. *Spectral methods*. Springer.

[59] Zayernouri, M., and Karniadakis, G. E., 2013. "Fractional Sturm-Liouville eigen-problems: theory and numerical approximations". *J. Comp. Physics,* **47-3**, pp. 2108–2131.

[60] Zayernouri, M., Ainsworth, M., and Karniadakis, G. E.,

2015. "Tempered fractional sturm–liouville eigenproblems". *SIAM Journal on Scientific Computing,* **37**(4), pp. A1777–A1800.

[61] Lischke, A., Zayernouri, M., and Zhang, Z. "Spectral and spectral element methods for fractional advection–diffusion–reaction equations". *Handbook of Fractional Calculus with Applications, Numerical Methods*.

[62] Lischke, A., Zayernouri, M., and Karniadakis, G. E., 2017. "A Petrov–Galerkin spectral method of linear complexity for fractional multiterm ODEs on the half line". *SIAM Journal on Scientific Computing,* **39**(3), pp. A922–A946.

[63] Suzuki, J. L., Zayernouri, M., Bittencourt, M. L., and Karniadakis, G. E., 2016. "Fractional-order uniaxial visco-elasto-plastic models for structural analysis". *Computer Methods in Applied Mechanics and Engineering,* **308**, pp. 443–467.

[64] Suzuki, J. L., and Zayernouri, M., 2018. "An automated singularity-capturing scheme for fractional differential equations". *arXiv preprint arXiv:1810.12219*.

[65] Samiee, M., Zayernouri, M., and Meerschaert, M. M., 2019. "A unified spectral method for PDEs with two-sided derivatives; part I: a fast solver". *Journal of Computational Physics,* **385**, pp. 225–243.

[66] Samiee, M., Kharazmi, E., and Zayernouri, M., 2017. "Fast spectral methods for temporally-distributed fractional PDEs". In *Spectral and High Order Methods for Partial Differential Equations ICOSAHOM 2016*. Springer, pp. 651–667.

[67] Samiee, M., Zayernouri, M., and Meerschaert, M. M., 2019. "A unified spectral method for FPDEss with two-sided derivatives; part II: Stability, and error analysis". *Journal of Computational Physics,* **385**, pp. 244–261.

[68] Samiee, M., Kharazmi, E., Zayernouri, M., and Meerschaert, M. M., 2018. "Petrov-Galerkin method for fully distributed-order fractional partial differential equations". *arXiv preprint arXiv:1805.08242*.

[69] Kharazmi, E., Zayernouri, M., and Karniadakis, G. E., 2017. "Petrov–Galerkin and spectral collocation methods for distributed order differential equations". *SIAM Journal on Scientific Computing,* **39**(3), pp. A1003–A1037.

[70] Kharazmi, E., Zayernouri, M., and Karniadakis, G. E. "A Petrov–Galerkin spectral element method for fractional elliptic problems". *Computer Methods in Applied Mechanics and Engineering,* **324**.

[71] Kharazmi, E., and Zayernouri, M., 2018. "Fractional pseudo-spectral methods for distributed-order fractional PDEs". *International Journal of Computer Mathematics*, pp. 1–22.

[72] Kharazmi, E., and Zayernouri, M., 2019. "Fractional sensitivity equation method: Application to fractional model construction". *Journal of Scientific Computing,* **80**(1), pp. 110–140.

[73] Rizzi, F., Najm, H. N., Debusschere, B. J., Sargsyan, K., Salloum, M., Adalsteinsson, H., and Knio, O. M., 2012. "Uncertainty quantification in md simulations. part I: Forward propagation". *Multiscale Modeling & Simulation,* **10**(4), pp. 1428–1459.

[74] Miller, K. S., and Ross, B., 1993. *An Introduction to the Fractional Calculus and Fractional Differential Equations*. New York, NY:John Wiley and Sons, Inc.

[75] Podlubny, I., 1999. *Fractional Differential Equations*. San Diego, CA, USA: Academic Press.

[76] Atanackovic, T. M., Pilipovic, S., Stankovic, B., and Zorica, D., 2014. *Fractional calculus with applications in mechanics: vibrations and diffusion processes*. John Wiley & Sons.

[77] Afzali, F., Kapucu, O., and Feeny, B. F., 2016. "Vibrational analysis of vertical-axis wind-turbine blades". In ASME 2016 International Design Engineering Technical Conferences and Computers and Information in Engineering Conference. American Society of Mechanical Engineers.

[78] Afzali, F., Acar, G. D., and Feeny, B. F., 2017. "Analysis of the periodic damping coefficient equation based on Floquet theory". In ASME 2017 International Design Engineering Technical Conferences and Computers and Information in Engineering Conference, American Society of Mechanical Engineers, pp. V008T12A050–V008T12A050.

[79] de Moraes, E. A. B., Zayernouri, M., and Meerschaert, M. M. "An integrated sensitivity-uncertainty quantification framework for stochastic phase-field modeling of material damage". *Int. J. Numerical Methods in Engineering (submitted)*.

[80] Zamani, V., Kharazmi, E., and Mukherjee, R., 2015. "Asymmetric post-flutter oscillations of a cantilever due to a dynamic follower force". *Journal of Sound and Vibration,* **340**, pp. 253–266.

[81] Varghaei, P., Kharazmi, E., Suzuki, J. L., and Zayernouri, M. "Nonlinear vibration of fractional viscoelastic cantilever beam: Application to structural health monitoring". *ASME Journal of Vibration and Acoustics (submitted)*.

[82] Ari, M., Faal, R. T., and Zayernouri, M., 2019. "Vibrations suppression of fractionally damped plates using multiple optimal dynamic vibration absorbers". *International Journal of Computer Mathematics*, pp. 1–24.

[83] Sapmaz, A., Acar, G. D., and Feeny, B. F., 2019. "Approximate general responses of tuned and mistuned 4-degree-of-freedom systems with parametric stiffness". In *Topics in Modal Analysis & Testing, Volume 9*. pp. 315–324.

[84] Loéve, M., 1977. *Probability Theory*. New York, Springer-Verlag.

[85] Su, C. H., and Lucor, D., 2006. "Covariance kernel representations of multidimensional second-order stochastic processes". *J. Comput. Phys.,* **217**(1), pp. 82–99.

[86] Oksendal, B., 1998. *Stochastic Differential Equations*. Springer-Verlag.

[87] Foo, J., Wan, X., and Karniadakis, G. E., 2008. "The multi-element probabilistic collocation method (ME-PCM): Error analysis and applications". *J. Comput. Phys.,* **227**, pp. 9572–9595.

[88] Barthelmann, V., Novak, E., and Ritter, K., 2000.

"High dimensional polynomial interpolation on sparse grids". *Advances in Computational Mathematics,* **12**(4), pp. 273–288.

[89] Novak, E., and Ritter, K., 1999. "Simple cubature formulas with high polynomial exactness". *Constructive approximation,* **15**(4), pp. 499–522.

[90] Novak, E., and Ritter, K., 1996. "High dimensional integration of smooth functions over cubes". *Numerische Mathematik,* **75**(1), pp. 79–97.

[91] Ervin, V. J., and Roop, J. P., 2007. "Variational solution of fractional advection dispersion equations on bounded domains in R^d". *Numerical Methods for Partial Differential Equations,* **23**(2), p. 256.